

SCIENTIFIC REPORTS



OPEN

Synthesis of prenylated flavonols and their potents as estrogen receptor modulator

Zhenru Tao^{1,2}, Juan Liu^{1,2}, Yueming Jiang¹, Liang Gong¹ & Bao Yang¹

Prenylated flavonols are known as phytoestrogen and have good bioactivities. However, their abundances in nature are pretty low. It is required to find an efficient synthesis technique. Icarin is a prenylated flavonol glycoside with low cost. It can be used to synthesize different prenylated flavonols. A combination of cellulase and trifluoacetic acid hydrolysis could effectively remove rhamnose and glucose from icariin. Icaritin, anhydroicaritin and wushanicaritin were the leading prenylated flavonol products. Their affinities to estrogen receptors α and β were predicted by docking study. The weak affinity of wushanicaritin indicated that prenyl hydroxylation impaired its affinity to estrogen receptor β . The prenyl cyclization led to a loss of affinity to both receptors. The interactions between icaritin and ligand binding cavity of estrogen receptor β were simulated. π - π stacking and hydrophobic forces were predicted to be the dominant interactions positioning icaritin, which induced the helix (H12) forming an activated conformation.

Prenylated flavonoids are an important sub-class of flavonoids, which combine a flavonoid skeleton with a lipophilic prenyl side chain¹. Even though flavonoids are widely present at a high level in nature², the levels of prenylated flavonoids are usually much lower. Prenylated flavonoids have been documented to be more bioactive than their flavonoid precursors, as prenylation increases the lipophilicity of flavonoids, leading to a higher permeability and bioavailability *in vivo*^{3,4}. For instance, 8-prenyl quercetin shows a higher cellular uptake and a lower efflux than quercetin in Caco-2 and C2C12 myotube cells. 8-Prenyl substitution also enhances the bioavailability of quercetin in different tissues *in vivo*⁵. Prenylated flavonoids possess a wide variety of bioactivities, such as estrogenic activity, immunomodulatory activity, anticancer activity and antioxidant activity^{6,7}.

Icaritin is a monoprenylated flavonol with 4'-methoxyl. It has been documented to have osteoblastic and neuroprotective activities^{8,9}. It can reduce the incidence of steroid-associated osteonecrosis in rabbit with inhibition of both intravascular thrombosis and extravascular lipid deposition for maintaining the integrity of intrasosseous vasculature¹⁰. The anti-breast cancer activity of icaritin remains confused. Icaritin at 5 μ M can inhibit the proliferation of breast cancer stem/progenitor cells even better than tamoxifen¹¹. However, a proliferation stimulatory effect has been observed for icaritin and desmethylcaritin in MCF-7 cells¹². Moreover, icaritin shows anti-inflammatory activity and inhibitory activities against other cancer cells¹³.

There are two classes of estrogen receptors, α and β . They are expressed in different tissues. Estrogen receptor α regulates the proliferation and differentiation of breast cancer cells. However, estrogen receptor β antagonizes the activities of estrogen receptor α , inhibiting carcinogenesis and tumor progression¹⁴. Estrogen receptor β expression is positively correlated with an improved clinical response to therapy and its loss is considered as an important step of cancer progression¹⁵. Therefore, it is of interest to find a selective estrogen receptor modulatory agent. As prenylated flavonols are potent phytoestrogens, it is worthy to find a selective estrogen receptor modulatory agents from this class of chemicals. However, due to their limited abundances in nature, it is required to develop an efficient synthesis technique. Though *Epimedium* genus is a good source of icaritin derivatives, the icaritin level is very low when determined by HPLC-MS¹⁶. As icariin is abundant in plants of *Epimedium* genus, using it as initial substrate to synthesize icaritin and its derivatives can be a possible way.

¹Key Laboratory of Plant Resources Conservation and Sustainable Utilization, Guangdong Provincial Key Laboratory of Applied Botany, South China Botanical Garden, Chinese Academy of Sciences, Guangzhou, 510650, China.

²University of Chinese Academy of Sciences, Beijing, 100049, China. Zhenru Tao and Juan Liu contributed equally to this work. Correspondence and requests for materials should be addressed to B.Y. (email: 156779996@qq.com)

Experimental section

Chemicals. Icariin, β -dextranase, β -glucosidase were purchased from Solarbio (Beijing, China). Cellulase was obtained from Yakult pharmaceutical Industry Co., LTD (Tokyo, Japan). HPLC grade acetonitrile was purchased from ANPEL Laboratory Technologies Inc. (Shanghai, China).

Synthesis of icaritin, anhydroicaritin and wushanicaritin. *Enzyme hydrolysis to remove glucoside.* Icariin (100 mg) were added into 25 ml of water. Five milligrams of enzymes were added to start the hydrolysis reaction at 37 °C for 2.5 h. The reaction products were extracted by acetyl acetate. The extract was dried by a vacuum rotary evaporator and redissolved in methanol. The products were qualified and quantified by ultra-performance liquid chromatography.

The effects of temperature, time and enzyme type were investigated. Three enzymes, including β -dextranase, β -glucosidase and cellulase, were tested to compare their hydrolysis efficiencies. When analysing the effect of temperature, 20, 37, 60 and 80 °C were used. The time were set as 1.5, 2.5, 3.5 and 4.5 h, respectively.

Acid hydrolysis to remove rhamnoside. Icariin (100 mg) were suspended in 25 ml of water. Trifluoacetic acid (TFA) was added to a final concentration of 2 M. The hydrolysis was conducted at 60 °C for 1 h. The reaction products were extracted by acetyl acetate. The extract was dried by vacuum rotary evaporator and redissolved in methanol. The products were qualified and quantified by ultra-performance liquid chromatography.

Combination of cellulase and TFA hydrolysis. Hydrolysis by cellulase first and then TFA: Icariin (100 mg) were added into 25 ml of water. Five milligrams of cellulase were added to start the hydrolysis reaction at 37 °C for 2.5 h. Then TFA was added to a final concentration of 2 M. The hydrolysis was conducted at 60 °C for 1 h. The reaction products were extracted by acetyl acetate. The extract was dried by vacuum rotary evaporator and redissolved in methanol. The products were qualified and quantified by ultra-performance liquid chromatography.

Hydrolysis by TFA first and then cellulase: Icariin (100 mg) were added into 25 ml of water. TFA was added to a final concentration of 2 M. The hydrolysis was conducted at 60 °C for 1 h. The hydrolysates were dried by vacuum rotary evaporator. Deionized water was added and dried again. This step was repeated for four times to completely remove acid. The dry products were redissolved in 25 ml of water. Five milligrams of cellulase were added to start the hydrolysis at 37 °C for 2.5 h. The reaction products were extracted by acetyl acetate. The extract was dried by vacuum rotary evaporator and redissolved in methanol. The products were qualified and quantified by ultra-performance liquid chromatography.

Preparation and identification of the reaction products. The enzymatic products were purified by semi-preparative reversed-phase liquid chromatography. 1.5 g of reaction products were loaded into a column with 15 × 460 mm. Methanol and water were used for elution. The column was equilibrated at 10% methanol for 12 min; 12–52 min, 75% methanol; 52–92 min, 80% methanol; 92–132 min, 85% methanol; 132–172 min, 90% methanol; 172–212 min, 100% methanol. The flow rate is 10 ml/min. The structures of the products were characterized by nuclear magnetic resonance (NMR) spectroscopy and mass spectrometry (MS) (Bruker AVIII, 500 MHz). The purified products were vacuum evaporated to dryness, dissolved in methanol-*d*₄ or acetone-*d*₆. 1D and 2D NMR spectra were recorded.

UPLC and UPLC-MS/MS analyses of reaction products. The analyses of reaction products and determination of conversion rate were performed on an Agilent 1260 Infinity UPLC system (Agilent Technologies, Germany)¹⁷. The analyses were performed on an Agilent ZORBAX SB-C18 column (3.0 × 100 mm, 1.8 μ m). The flow rate was 0.3 ml/min, the column temperature was set at 40 °C, and the injection volume was 10 μ l. The chromatogram was monitored at 280 nm. The mobile phases comprised solvents A (ultrapure water) and B (methanol). The elution program was as follows: 0–30 min, 5–100% B; 30–40 min, 100% B¹⁸.

UPLC-MS/MS was analysed on a maXis LC-ESI-QTOF-MS system (Bruker, Germany) equipped with an Agilent ZORBAX SB-C18 column (3.0 × 100 mm, 1.8 μ m). The elution program was the same as UPLC analysis. Ionization of the analytes was achieved by using electron spray ionization interface in negative mode. The collision voltage was 10 eV. Mass scan was set in the range of *m/z* 50–1000. The daughter ions were monitored at a collision voltage range of 28–42 eV¹⁹.

Binding affinity prediction by molecular docking. The X-ray structure of estrogen receptor α and β in complex with agonist (2R,3S,4R)-(4-hydroxyphenyl)-6-hydroxy-cyclopentyl[*c*]3,4-dihydro-2H-1-benzopyran (PDB id: 2i0j and 2i0g) were used as the templates²⁰. Autodocktools (version 1.5.6rc3) was used to dock estrogen receptor α/β and the tested chemicals²¹. The protein was checked for any missing atoms, removed water and added hydrogen. The ligand was drawn and saved as a mol2 file. It was opened in autodocktools and saved as PDBQT file. A grid was generated for protein with the ligand centered. Genetics algorithm was used for docking²². The binding affinity was recorded to evaluate the potential to be estrogen receptor agonist.

Results and Discussion

Synthesis of anhydroicaritin, icaritin and wushanicaritin. *Enzyme hydrolysis of icariin.* Three enzymes, including cellulase, β -glucosidase and β -dextranase, were used to hydrolyse icariin, respectively. There was only one product generated after enzyme hydrolysis (Fig. 1). It was purified and subjected to NMR analysis. The ¹H and ¹³C chemical shifts of this chemical are listed in Table 1S and Fig. 2S. When comparing with icariin (1, Fig. 1S), the missing of glucosyl signals indicated the loss of this moiety. An upfield shift of H-6 was observed at 6.26 ppm. The chemical shifts of C-7 and C-8 were changed accordingly. The rhamnosyl with anomeric signals (5.40/103.7 ppm) was detected²³. It confirmed that these enzymes could not degrade this unit. The above information confirmed the presence of **baohuoside I** (2).

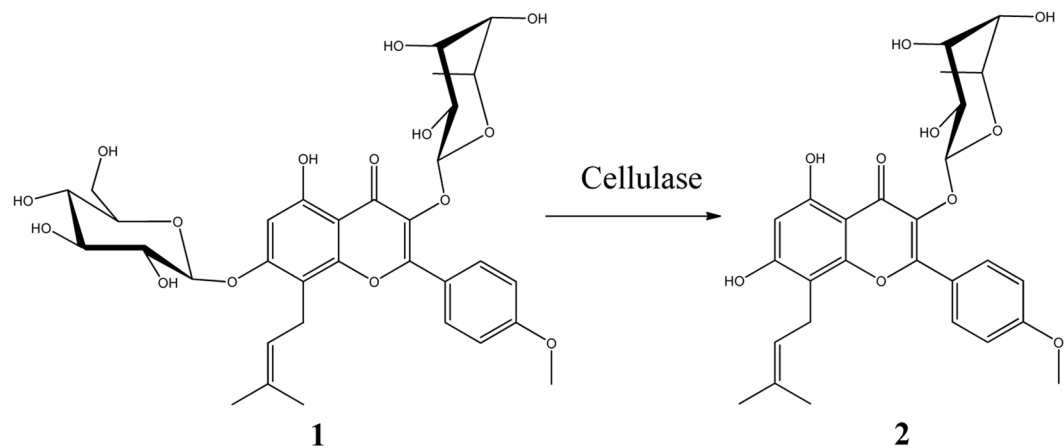


Figure 1. The reaction product of icariin hydrolysed by cellulase at 37 °C for 2.5 h. Yield of 2, 94.8%.

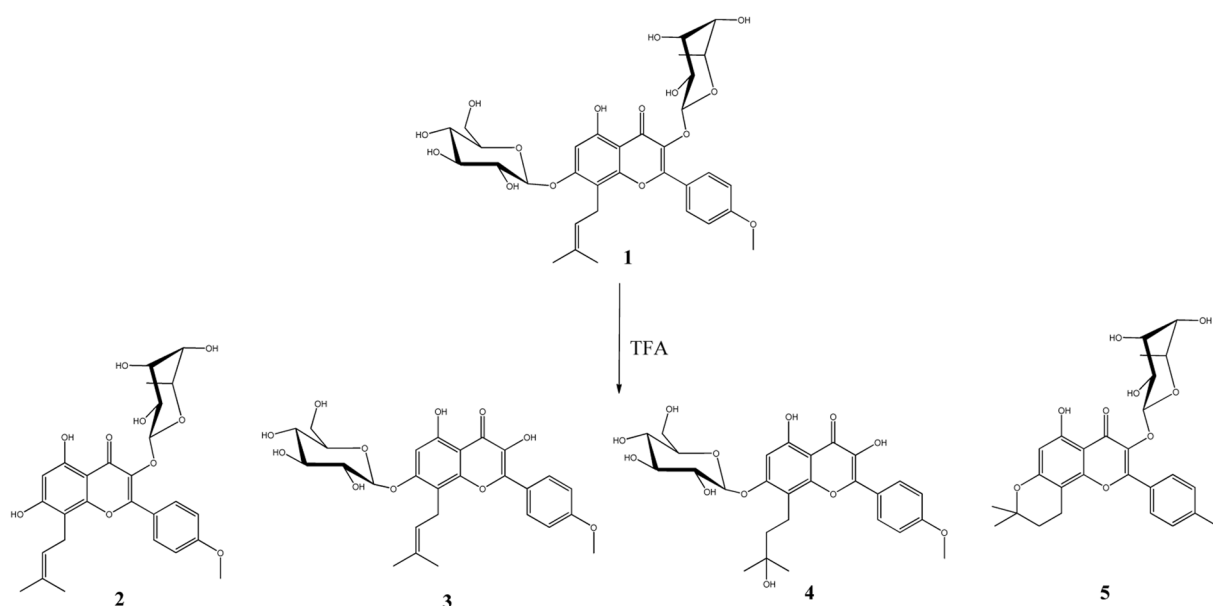


Figure 2. The reaction products of icariin hydrolysed by TFA at 60 °C for 1.0 h. Yields of 2, 3.5%; 3, 49.3%; 4, 32.7%; 5, 1.6%.

UPLC-QTOF-MS is used to determine the precise molecular weight and fragmentation pattern of baohuoside I in negative mode (Table 2S). A parent ion $[M-H]^-$ at m/z 513.1761 was observed. m/z 367.1112 indicated the loss of rhamnosyl. Two peaks at m/z 323.0921 and 311.0573 suggested the cleavage of prenyl and loss of C_3H_6 and C_4H_8 moieties, respectively²⁴.

Though β -glucosidase has been reported to be effective in hydrolysis of icariin²⁵, its effectiveness was much lower than cellulase in this work (Fig. 10S). The icariside I yield reached 94.8% by cellulase hydrolysis, while the yield was lower than 50% when β -glucosidase or β -dextranase was used. Temperature influenced the glucosyl cleavage to a certain extent. The highest yield of icariside I was obtained when 37 or 60 °C were applied. It indicated a broad temperature tolerance of cellulase. Out of this range made the hydrolysis efficiency decreased sharply. Hydrolysis time showed a weak effect on icariside I yield. 2.5 h was the optimal value. Further extension of reaction time led to a slight decrease of icariside I, which might be due to the degradation.

Acid hydrolysis of icariin. Icariin was hydrolysed by TFA and four products were detected (Fig. 2). They were purified by C-18 column and identified by UPLC-MS/MS and NMR. Please see Table 2S and Figs 3S–5S. Chemical 3 showed a parent ion $[M-H]^-$ at m/z 529.1765, which was equal to the molecular weight of icariside I²⁶. The fragments also confirmed this identification. A fragment at m/z 473.1316 suggested the breakage of prenyl between C-1 and C-2. The loss of glucosyl was observed by the peak at m/z 367.1115. The anomeric signals of

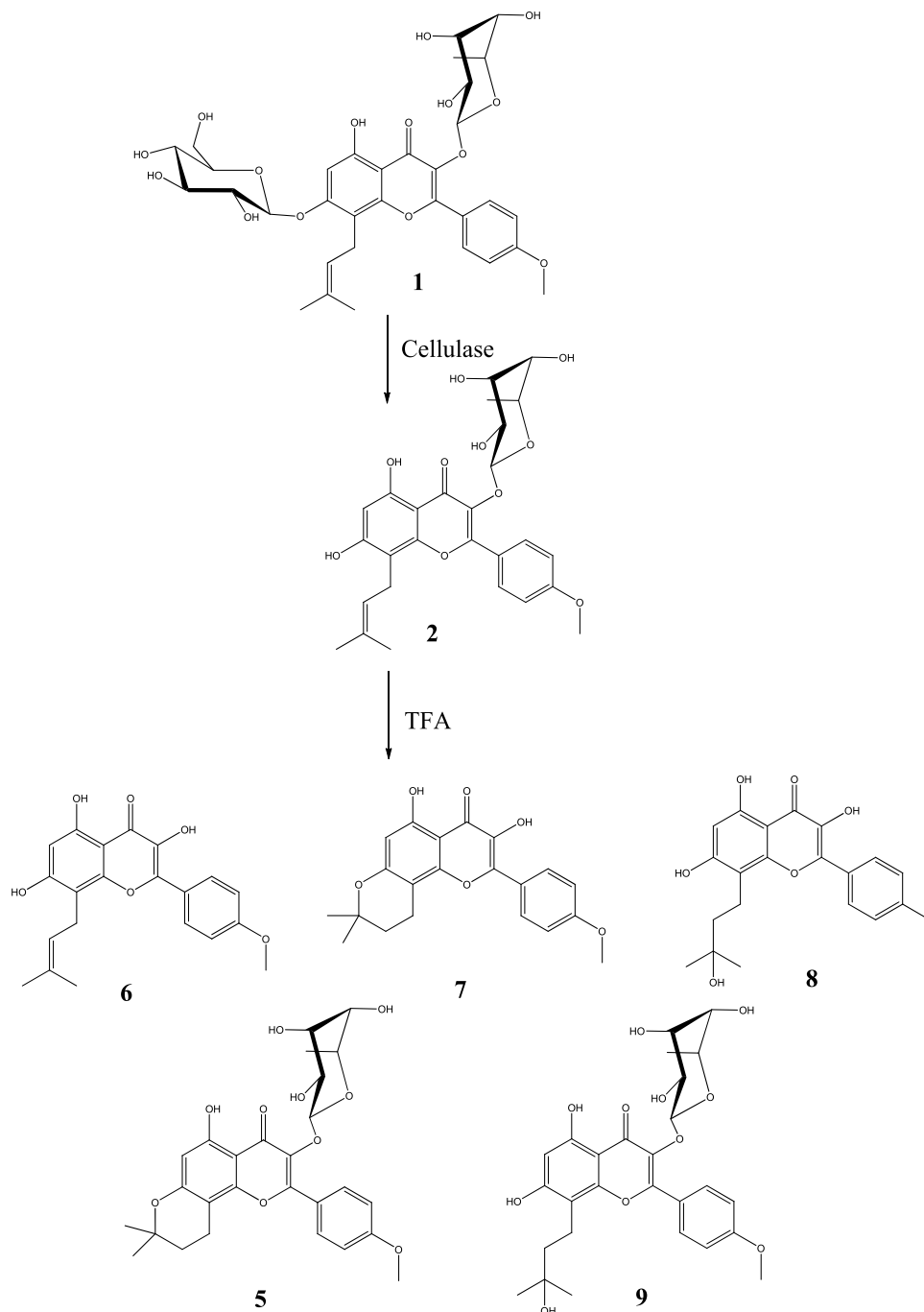


Figure 3. The reaction products of icariin hydrolysed by cellulase firstly and then TFA. Yields of **5**, 10.5%; **6**, 61.1%; **7**, 12.2%; **8**, 3.7%; **9**, 7.6%.

rhamnosyl (5.40/103.7 ppm) were not detected. It indicated the removal of rhamnosyl from icariin. By comparison with NMR signals of icariin, **3** was identified as icariside I.

Chemical **4** was analysed to have a parent ion $[M-H]^-$ at m/z 547.1892. It was 18 larger than icariside I (**3**), which implicated the presence of H_2O . In NMR spectra, a quaternary carbon signal C-3'' at 71.7 ppm and C-2'' signal at 18.8 ppm further indicated the hydration of prenyl. Through comparing with NMR signals of icariside I and literatures²⁷, chemical **4** was identified as maohuoside A.

A minor amount of chemical **5** was detected. It had a parent ion $[M-H]^-$ at m/z 513.1759. The fragment ion at m/z 367.1115 indicated the loss of rhamnosyl. The anomeric signals of 5.44/102.2 ppm in NMR spectra also confirmed the presence of rhamnosyl. A cyclization between C-3'' of prenyl and 6-OH was observed by the NMR signals 2.84/16.8 (H-1''/C-1''), 1.88/32.1 (H-2''/C-2''), 77.5 (C-3''), 1.36/26.4 (H-4''/C-4'' and H-5''/C-5''). Therefore, chemical **5** was identified as anhydroicaritin 3-O-rhamnoside.

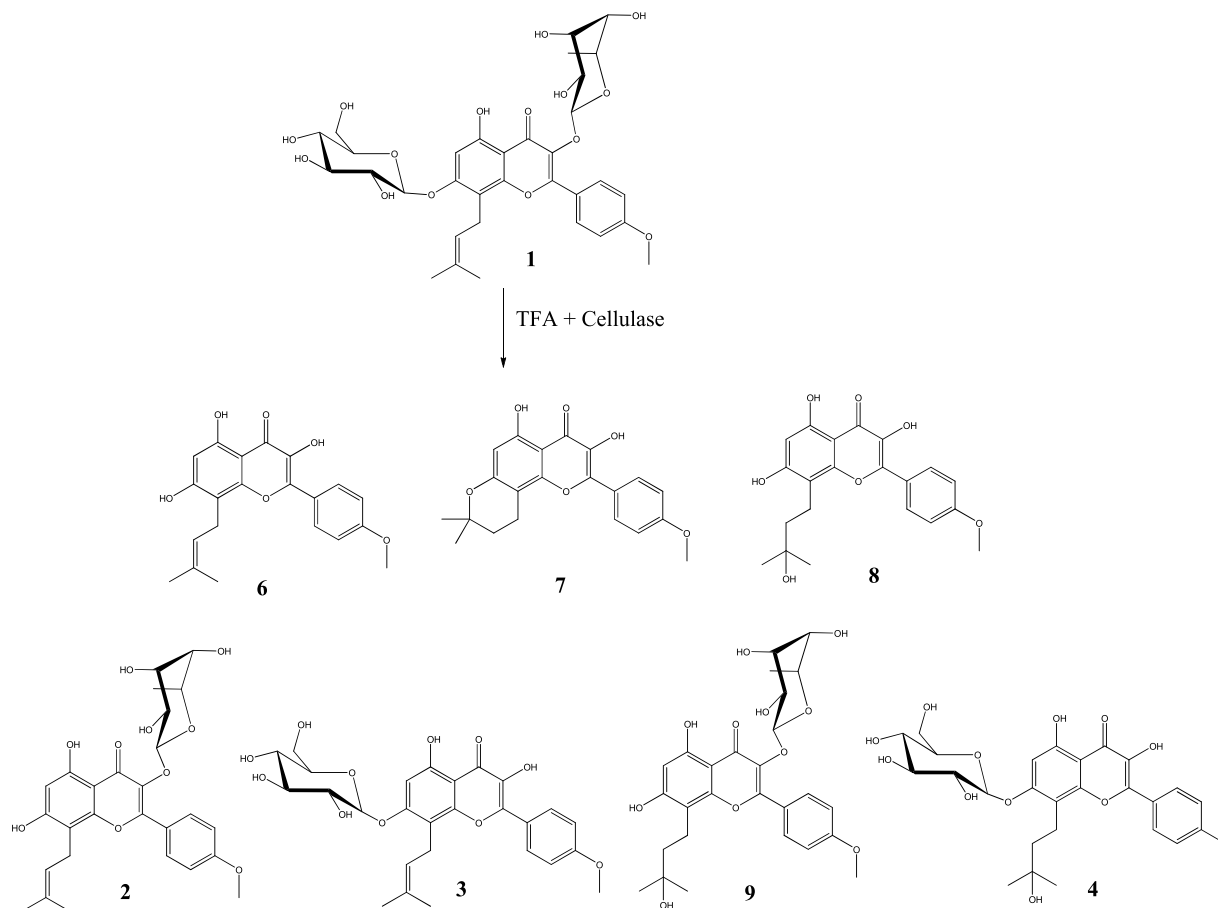


Figure 4. The reaction products of icariin hydrolysed by TFA firstly and then cellulase. Yields of **2**, 10.5%; **3**, 7.3%; **4**, 4.4%; **6**, 28.8%; **7**, 16.9%; **8**, 25.3%; **9**, 2.1%.

The four chemicals generated by TFA hydrolysis of icariin were compared. **2** and **5** contained rhamnosyl, but no glucosyl, while **3** and **4** contained glucosyl but no rhamnosyl. Rhamnosyl was easier to be cleaved than glucosyl by acid. In acidic conditions, the prenyl was unstable and readily to be hydrated or cyclized. No products without both rhamnosyl and glucosyl were detected. It indicated that TFA hydrolysis could not directly generate icaritin. Therefore, combination of cellulase and TFA hydrolysis was carried out in the following work.

Combination of cellulase and acid hydrolysis. When icariin was hydrolysed by cellulase firstly and then by TFA, five main products were detected (Figure 11S). The reaction route and products are shown in Fig. 3. Chemical **6** was the dominant product which had a parent ion $[M-H]^-$ at m/z 367.1142. No rhamnosyl and glucosyl signals were observed in the NMR signals (Fig. 6S). Their losses led to the upfield movements of H-6, C-2, C-4 and downfield shift of C-3. The fragment ion at m/z 352.0974 was due to the loss of methyl. m/z 311.0601 was produced by the cleavage of prenyl between C-1'' and C-2''. These information confirmed that chemical **6** was icaritin¹⁰.

Chemical **7** had a parent ion $[M-H]^-$ at m/z 367.1135. It was consistent to the parent ion of icaritin. By comparing the NMR signals (Figure 7S), the double bond of prenyl was not found in chemical **7**. The quaternary carbon signal of 77.7 ppm at C-3'' and two-proton signal of 1.95 ppm at H-2'' suggested a cyclization between C-3'' and 7-OH. Therefore, chemical **7** was identified as anhydroicaritin.

Chemical **8** had a parent ion $[M-H]^-$ at m/z 385.1165. It was 18 more than that of icaritin. The quaternary carbon signal of 71.7 ppm at C-3'' and 2 H signals of 2.90–2.95 ppm at H-2'' suggested the hydration of icaritin (Table 1S and Figure 8S). It was called wushanicaritin²⁸. Chemical **9** was identified to be 3-O-rhamnosyl wushanicaritin by the parent ion $[M-H]^-$ at m/z 531.1246 and NMR signals (Figure 9S).

When icariin was hydrolysed by TFA firstly and then cellulase, seven chemicals were produced as the main reaction products (Fig. 4, Figure 12S). These chemicals were identified as baohuoside I (**2**), icaritin (**6**), anhydroicaritin (**7**), wushanicaritin (**8**) and wushanicaritin 3-O-rhamnoside (**9**). Anhydroicaritin 3-O-rhamnoside (**5**) was not detected as a product. The yields of icaritin, anhydroicaritin and wushanicaritin were calculated to be 28.8%, 16.9% and 25.3%, respectively.

When icariin was hydrolysed by cellulase firstly and then TFA, baohuoside I (**2**) was not detected in the products. It was cyclized into anhydroicaritin 3-O-rhamnoside (**5**). The yields of icaritin, anhydroicaritin and

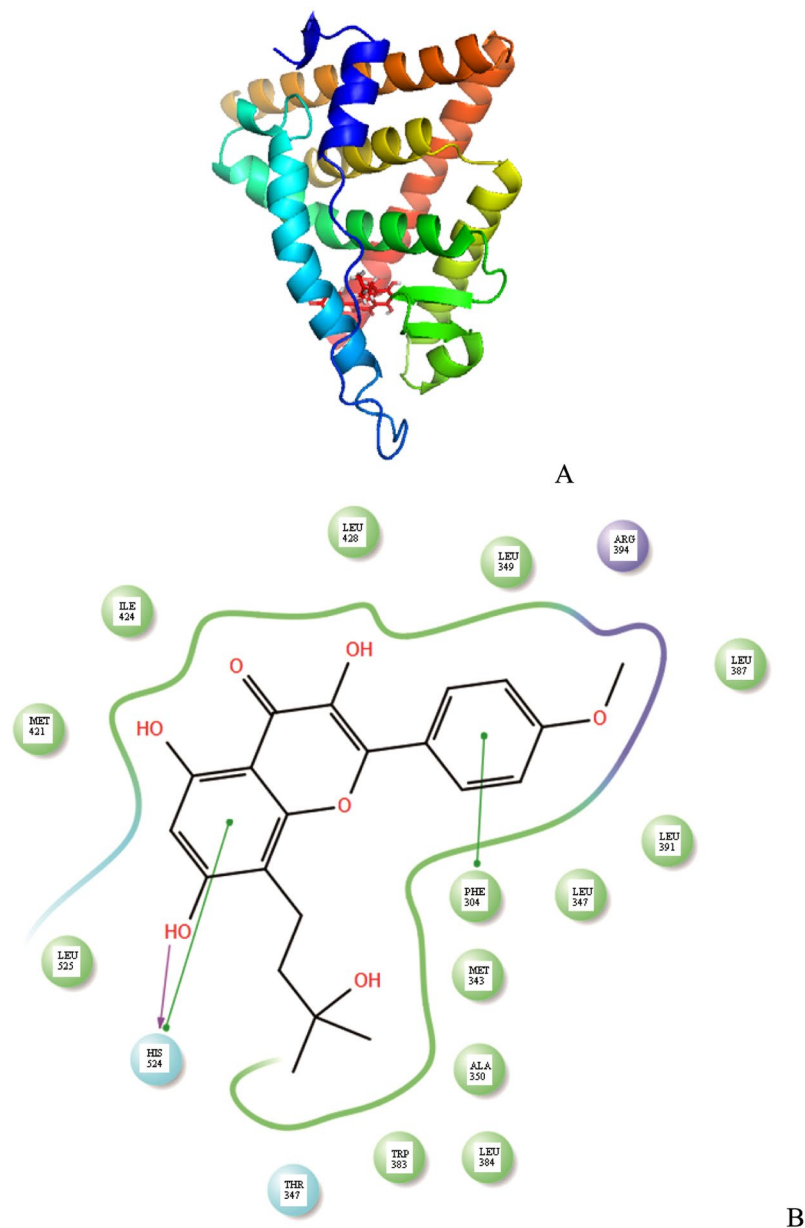


Figure 5. Docking simulation of estrogen receptor α in complex with wushanicaritin. (A) The steric structure of complex; (B) The interactions between amino acids and wushanicaritin.

wushanicaritin were calculated to be 61.1%, 12.2% and 3.7%, respectively. Therefore, hydrolysis by cellulase firstly and then TFA would be a good choice for icaritin preparation.

Docking study. Molecular docking simulation was performed for icaritin, anhydroicaritin and wushanicaritin, in order to predict the estrogen receptor α/β -agonist interactions. The most favorable docking conformation was retrieved from calculation. As shown in Table 3S, in the docking model, wushanicaritin showed high binding affinities to estrogen receptors α (-8.48 kcal/mol) and β (-7.97 kcal/mol). Icaritin only exhibited a good binding affinity to estrogen receptor β (-9.46 kcal/mol). Anhydroicaritin showed poor binding affinities to both estrogen receptors. Icaritin was predicted to have a good selectivity due to its specific binding affinity to estrogen receptor β .

Figure 5 shows the docking conformation of estrogen receptor α and wushanicaritin. The ligand binding domain of estrogen receptor α comprises of three anti-parallel α -helices layers, including a central layer and two outside layers²⁹. The residues Met343, Leu346, Leu349, Ala350, Trp383, Leu384, Leu391, Leu387, Met421, Ile424, Leu428 and Leu525 are predicted to be involved in the positioning of wushanicaritin by hydrophobic forces. Phe404 was predicted to interact with wushanicaritin by π - π stacking. His524 was predicted to generate a hydrogen bond and π - π stacking interaction to stabilize wushanicaritin. The conformation of H12 in the complex determines the binding possibility of coactivator to activate function domain (AF-2). In the estrogen receptor α /

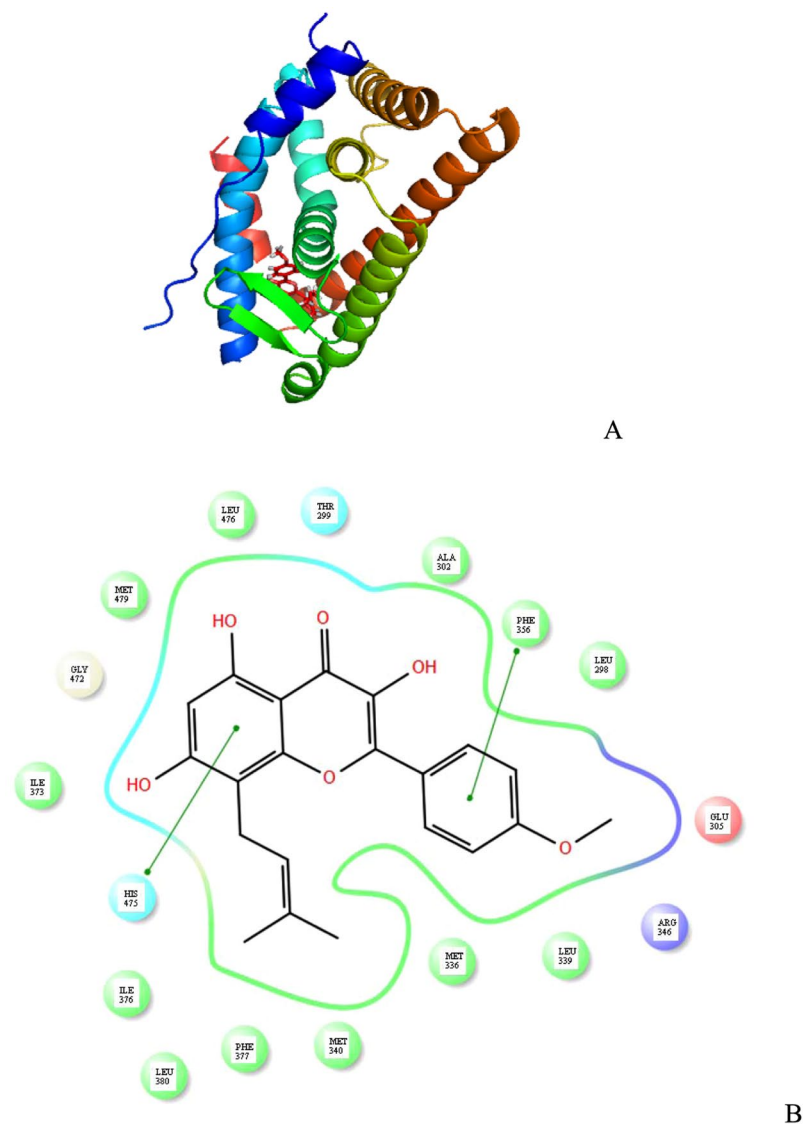


Figure 6. Docking simulation of estrogen receptor β in complex with icaritin. (A) The steric structure of complex; (B) The interactions between amino acids and icaritin.

wushanicaritin complex, H12 was predicted to seal the ligand-binding cavity and to generate a competent AF-2 that could interact with coactivator. This could be helpful to explain how wushanicaritin acted as an agonist.

Figure 6 shows the predicted conformation of estrogen receptor β in complex with icaritin. Estrogen receptor β is present similarly to estrogen receptor α as a sandwich made by a central layer and two outside layers. H12 forms a lid on the binding cavity. π - π stacking interaction was observed by residues His475 and Phe356. No hydrogen bonds were detected to position icaritin in the predicted conformation. Hydrophobic forces from Leu298, Ala302, Leu476, Met479, Ile373, Ile376, Leu380, Phe377, Met340, Met336 and Leu339 were predicted to be involved in stabilizing icaritin.

Conclusions

A combination of cellulase and TFA hydrolysis was confirmed to be an efficient technique to synthesize icaritin, wushanicaritin and anhydroicaritin. This technique extended the application of cellulase in icaritin preparation and made production of three aglycones in one pot possible³⁰. It was easy to carry out and to produce at a large scale when comparing synthesis from kaempferol³¹. Icaritin, wushanicaritin and anhydroicaritin are good drug candidates due to their good performance against cancer and osteoporosis. Developing a cost effective technique is of great interest for medicine industry. As the prenylation pattern produced a significant effect on the activity performance, it is required to conduct more bioactivity evaluations, including the estrogen receptor modulatory mechanisms *in vitro* and *in vivo*, to understand the potencies of these chemicals in medicines. Some bioactivities, like anti-breast cancer, anti-osteoporosis or memory improving capabilities, should be evaluated, as estrogen receptor modulatory behaviours are involved in the mechanism of action.

References

1. Toume, K. *et al.* Prenylated flavonoids and resveratrol derivatives isolated from *Artocarpus communis* with the ability to overcome TRAIL resistance. *J Nat Prod* **78**, 103–110, <https://doi.org/10.1021/np500734t> (2015).
2. Wen, L. *et al.* Structure, bioactivity, and synthesis of methylated flavonoids. *Ann N Y Acad Sci* **1398**, 120–129, <https://doi.org/10.1111/nyas.13350> (2017).
3. Chen, Y., Zhao, Y. H., Jia, X. B. & Hu, M. Intestinal absorption mechanisms of prenylated flavonoids present in the heat-processed *Epimedium koreanum* Nakai (Yin Yanghuo). *Pharm Res* **25**, 2190–2199, <https://doi.org/10.1007/s11095-008-9602-7> (2008).
4. Botta, B., Vitali, A., Menendez, P., Misiti, D. & Delle Monache, G. Prenylated flavonoids: Pharmacology and biotechnology. *Curr Med Chem* **12**, 713–739 (2005).
5. Mukai, R. *et al.* Prenylation enhances quercetin uptake and reduces efflux in Caco-2 cells and enhances tissue accumulation in mice fed long-term. *J Nutr* **143**, 1558–1564, <https://doi.org/10.3945/jn.113.176818> (2013).
6. Yang, X. M. *et al.* Prenylated flavonoids, promising nutraceuticals with impressive biological activities. *Trends Food Sci Tech* **44**, 93–104, <https://doi.org/10.1016/j.tifs.2015.03.007> (2015).
7. Sun, Y. J. *et al.* Prenylated flavonoids from the fruits of *Sinopodophyllum emodi* and their cytotoxic activities. *Rsc Adv* **5**, 82736–82742, <https://doi.org/10.1039/c5ra16136c> (2015).
8. Zhang, Z. K. *et al.* Icaritin requires phosphatidylinositol 3 kinase (PI3K)/Akt signaling to counteract skeletal muscle atrophy following mechanical unloading. *Sci Rep-Uk* **6**, <https://doi.org/10.1038/Srep20300> (2016).
9. Huang, J., Yuan, L., Wang, X., Zhang, T. L. & Wang, K. Icaritin and its glycosides enhance osteoblastic, but suppress osteoclastic, differentiation and activity *in vitro*. *Life Sci* **81**, 832–840, <https://doi.org/10.1016/j.lfs.2007.07.015> (2007).
10. Zhang, G. *et al.* A novel semisynthesized small molecule icaritin reduces incidence of steroid-associated osteonecrosis with inhibition of both thrombosis and lipid-deposition in a dose-dependent manner. *Bone* **44**, 345–356, <https://doi.org/10.1016/j.bone.2008.10.035> (2009).
11. Guo, Y. M., Zhang, X. T., Meng, J. & Wang, Z. Y. An anticancer agent icaritin induces sustained activation of the extracellular signal-regulated kinase (ERK) pathway and inhibits growth of breast cancer cells. *Eur J Pharmacol* **658**, 114–122, <https://doi.org/10.1016/j.ejphar.2011.02.005> (2011).
12. Wang, Z. Q. & Lou, Y. J. Proliferation-stimulating effects of icaritin and desmethylicaritin in MCF-7 cells. *Eur J Pharmacol* **504**, 147–153, <https://doi.org/10.1016/j.ejphar.2004.10.002> (2004).
13. Fu, B. S. *et al.* GRAM domain-containing protein 1A (GRAMD1A) promotes the expansion of hepatocellular carcinoma stem cell and hepatocellular carcinoma growth through STAT5. *Sci Rep-Uk* **6**, <https://doi.org/10.1038/Srep31963> (2016).
14. Stellato, C. *et al.* Identification of cytoplasmic proteins interacting with unliganded estrogen receptor and in human breast cancer cells. *Proteomics* **15**, 1801–1807, <https://doi.org/10.1002/pmic.201400404> (2015).
15. Sareddy, G. R. *et al.* Selective estrogen receptor beta agonist LY500307 as a novel therapeutic agent for glioblastoma. *Sci Rep-Uk* **6**, <https://doi.org/10.1038/Srep24185> (2016).
16. Li, H. F. *et al.* Qualitative and quantitative analyses of *Epimedium wushanense* by high-performance liquid chromatography coupled with diode array detection and electrospray ionization tandem mass spectrometry. *J Sep Sci* **34**, 1437–1446, <https://doi.org/10.1002/jssc.201000899> (2011).
17. Fu, C. L. *et al.* Structure, antioxidant and alpha-amylase inhibitory activities of longan pericarp proanthocyanidins. *J Funct Foods* **14**, 23–32, <https://doi.org/10.1016/j.jff.2015.01.041> (2015).
18. Feng, X., Ng, V. K., Mikš-Krajnik, M. & Yang, H. S. Effects of fish gelatin and tea polyphenol coating on the spoilage and degradation of myofibril in fish fillet during cold storage. *Food Bioprocess Tech* **10**, 89–102, <https://doi.org/10.1007/s11947-016-1798-7> (2017).
19. Wen, L. R. *et al.* Identification of phenolics in litchi and evaluation of anticancer cell proliferation activity and intracellular antioxidant activity. *Free Radical Bio Med* **84**, 171–184, <https://doi.org/10.1016/j.freeradbiomed.2015.03.023> (2015).
20. Norman, B. H. *et al.* Benzopyrans are selective estrogen receptor beta agonists with novel activity in models of benign prostatic hyperplasia. *J Med Chem* **49**, 6155–6157, <https://doi.org/10.1021/jm060491j> (2006).
21. Sanner, M. F. Python: A programming language for software integration and development. *J Mol Graph Model* **17**, 57–61 (1999).
22. Yang, X. M. *et al.* Regiospecific synthesis of prenylated flavonoids by a prenyltransferase cloned from *Fusarium oxysporum*. *Sci Rep-Uk* **6**, 24819, <https://doi.org/10.1038/srep24819> (2016).
23. Ferreira, J. C. *et al.* Isolation of a dihydrobenzofuran lignan, icaraside E-4, with an antinociceptive effect from *Tabebuia roseo-alba* (Ridley) Sandwith (Bignoniaceae) bark. *Arch Pharm Res* **38**, 950–956, <https://doi.org/10.1007/s12272-014-0468-4> (2015).
24. Xu, W. *et al.* LC-MS/MS method for the simultaneous determination of icaritin and its major metabolites in rat plasma. *J Pharmacol Biomed* **45**, 667–672, <https://doi.org/10.1016/j.jpba.2007.07.007> (2007).
25. Xia, Q. A. *et al.* Preparation of icaraside II from icaritin by enzymatic hydrolysis method. *Fitoterapia* **81**, 437–442, <https://doi.org/10.1016/j.fitote.2009.12.006> (2010).
26. Tu, Y., Zhao, L. H., Zhu, L., Wang, G. J. & Xiang, B. R. Simultaneous determination of acteoside, astragaloside IV and icaraside-I in the traditional Chinese medicinal preparation Shenbao by HPLC-MS. *Chromatographia* **64**, 453–458, <https://doi.org/10.1365/s10337-006-0053-1> (2006).
27. Jiang, F., Wang, X. L., Wang, N. L. & Yao, X. S. Two new flavonol glycosides from *Epimedium koreanum* Nakai. *J Asian Nat Prod Res* **11**, 401–409, <https://doi.org/10.1080/10286020902867151> (2009).
28. Li, H. F. *et al.* Antioxidant flavonoids from *Epimedium wushanense*. *Fitoterapia* **83**, 44–48, <https://doi.org/10.1016/j.fitote.2011.09.010> (2012).
29. Brzozowski, A. M. *et al.* Molecular basis of agonism and antagonism in the oestrogen receptor. *Nature* **389**, 753–758, <https://doi.org/10.1038/39645> (1997).
30. Park, J. S. *et al.* Statistically designed enzymatic hydrolysis for optimized production of icaraside II as a novel melanogenesis inhibitor. *J Microbiol Biotechnol* **18**, 110–117 (2008).
31. Mei, Q. G., Wang, C., Zhao, Z. G., Yuan, W. C. & Zhang, G. L. Synthesis of icaritin from kaempferol through regioselective methylation and para-Claisen-Cope rearrangement. *Beilstein J Org Chem* **11**, <https://doi.org/10.3762/bjoc.11.135> (2015).

Acknowledgements

We are grateful to the financial support from National Key Research and Development Program of China (2017YFD0401301), National Natural Science Foundation of China (31671906), Frontier Science Key Program of Chinese Academy of Sciences (QYZDB-SSW-SMC018), Guangdong Natural Science Fund for Distinguished Young Scholar (S2013050014131), Science and Technology Planning Project of Guangdong Province (2016A010105014 and 2017A020211030) and Youth Innovation Promotion Association of Chinese Academy of Sciences (2011252).

Author Contributions

Zhenru Tao, icaritin hydrolysis. Juan Liu, docking analysis. Yueming Jiang, experiment design and paper writing. Liang Gong, mass spectrometry analysis. Bao Yang, experiment design, results analyses and paper writing.

Additional Information

Supplementary information accompanies this paper at <https://doi.org/10.1038/s41598-017-12640-9>.

Competing Interests: The authors declare that they have no competing interests.

Publisher's note: Springer Nature remains neutral with regard to jurisdictional claims in published maps and institutional affiliations.



Open Access This article is licensed under a Creative Commons Attribution 4.0 International License, which permits use, sharing, adaptation, distribution and reproduction in any medium or format, as long as you give appropriate credit to the original author(s) and the source, provide a link to the Creative Commons license, and indicate if changes were made. The images or other third party material in this article are included in the article's Creative Commons license, unless indicated otherwise in a credit line to the material. If material is not included in the article's Creative Commons license and your intended use is not permitted by statutory regulation or exceeds the permitted use, you will need to obtain permission directly from the copyright holder. To view a copy of this license, visit <http://creativecommons.org/licenses/by/4.0/>.

© The Author(s) 2017